



## Reinvestigation of the $v_3\!-\!v_6$ Coriolis Interaction in Trifluoroiodomethane

Journal:	Physical Chemistry Chemical Physics
Manuscript ID	CP-ART-07-2024-002640.R1
Article Type:	Paper
Date Submitted by the Author:	24-Sep-2024
Complete List of Authors:	Bhujel, Arun; Texas Tech University, Chemistry and Biochemistry Akter, Salma; Texas Tech University, Chemistry and Biochemistry Ali, Muhammad; Texas Tech University, Chemistry and Biochemistry Park, G.; Texas Tech University, Chemistry and Biochemistry; Max Planck Institute for Multidisciplinary Sciences, Dynamics at Surfaces

SCHOLARONE™ Manuscripts

# Reinvestigation of the $\nu_3$ - $\nu_6$ Coriolis Interaction in Trifluoroiodomethane

Arun Bhujel, 1† Salma Akter, 1† Muhammad Qasim Ali, 1 G. Barratt Park 1,2\*

**Affiliations** 

<sup>1</sup>Department of Chemistry and Biochemistry, Texas Tech University, Lubbock, Texas 79409, United States

<sup>2</sup>Department of Dynamics at Surfaces, Max Planck Institute for Multidisciplinary Sciences, Göttingen 37077, Germany

†These authors contributed equally.

\*barratt.park@ttu.edu

#### **Abstract**

The lowest-frequency fundamental  $\nu_6$  of trifluoroiodomethane (CF<sub>3</sub>I) has never been directly observed and analyzed at high resolution in the gas phase. The  $\nu_6(e)$  level interacts with  $\nu_3(a_1)$  at 286.297 cm<sup>-1</sup> via a *b*-axis Coriolis interaction, which perturbs the rotational structure of both levels. In this work, we report low-*J* microwave transitions (for *J* ranging from 0–2) within the  $\nu_6$  vibrational level. The *l*-type doubling observed in our spectrum agreed poorly with the predictions of previously published models of the interacting  $\nu_3$ - $\nu_6$  levels, prompting us to refine the model. We performed *ab initio* anharmonic force-field calculations, which were used to constrain some of the parameters, and which served as a check on some of the floated parameters. We fit a dataset consisting of 3593 transitions, which combined our measurements with previous microwave, millimeter wave, and high-resolution infrared observations. A reasonable set of fit parameters is obtained with  $\nu_6 = 267.28$  cm<sup>-1</sup>, but we cannot rule out a lower value of  $\nu_6 = 261.5$  cm<sup>-1</sup> consistent with analyses of the vibrational level structure.

#### Introduction

Trifluoroiodomethane (CF<sub>3</sub>I) has potential as a more environmentally friendly alternative to Halon 1301 (CF<sub>3</sub>Br) as a fire suppressant, since its ozone depleting potential is lower by a factor of ~1000. Tes I has also been used in trifluoromethylation reactions and multiphoton dissociation experiments. The frequency of its lowest-lying fundamental,  $\nu_6$ (e) was the subject of some controversy in the early IR and Raman work because the  $\nu_6$  fundamental transition is relatively weak and is poorly resolved from the stronger  $\nu_3$ (a<sub>1</sub>) fundamental. 4-9 Values reported for the  $\nu_3$  —

 $v_6$  frequency difference range from 19–28 cm<sup>-1</sup>. A number of microwave studies have been reported on CF<sub>3</sub>I in its ground vibrational state.<sup>8,10-14</sup> A millimeter-wave study by Walters and Whiffen<sup>15</sup> led to the assignment of rotational transitions in the excited  $v_6$  and  $v_3$  vibrational levels and enabled a characterization of the *b*-axis Coriolis interaction between the  $v_6$  and  $v_3$  levels. This analysis favored a low value of  $v_3 - v_6 = 19 \pm 2$  cm<sup>-1</sup>. On the other hand, careful assessment of the vibrational level structure has led to a value of  $v_3 - v_6 = 24.8 \pm 1.5$  cm<sup>-1</sup>.<sup>16</sup>

Subsequent high-resolution spectroscopic investigations include a microwave study by Gerke and Harder<sup>17</sup> in which direct *l*-type doubling transitions are reported for the  $\nu_6$  level in the J=40–51 range. These authors reported parameters for the off-diagonal spin-rotation interaction with  $\Delta l = \Delta K = \pm 2$  selection rules. The hyperfine structure probed in this work is also highly sensitive to the *b*-axis Coriolis interaction with the  $\nu_3$  level, but the authors made no attempt to deperturb Coriolis contributions, using instead effective values for the  $q^+$  and  $q_J$  *l*-type doubling constants.

In another study by Willaert et al., 18 a high-resolution infrared spectrum of the  $v_3$ fundamental band was recorded at 0.001 cm<sup>-1</sup> resolution using synchrotron sources. These authors searched for the  $v_6$  fundamental but could not detect it due to its extremely weak transition strength. The authors estimated an upper limit of 7.5 m/mol for the integrated cross section of the  $v_6$  band. Three different fit models were used to interpret the results. In the preliminary analysis,  $v_3$  was considered to be an isolated state, and its perturbed rotational structure was fitted with the help of high-order centrifugal distortion parameters that effectively account for the Coriolis interaction with  $\nu_6$ . The Coriolis interaction was taken into account explicitly in two additional models, which were fit to combined datasets that included microwave and millimeter wave transitions<sup>15,17</sup> within modes  $v_3$  and  $v_6$  in addition to the  $v_3$  IR data. 18 In the first model, the  $v_6$  origin was fixed to the value reported by Walters and Whiffen  $^{15}$  and the  $A_6$  rotational constant was constrained to equal the  $A_3$  rotational constant. (Here, subscripts refer to the rotational parameters for the  $\nu_6$  and  $\nu_3$ fundamental vibrational levels, respectively.) In the second model, the  $v_6$  origin was fixed to the value reported by Bürger  $et\ al.^{16}$  Both fits required the inclusion of high-order  $C_B^I$  and  $C_B^K$  Coriolis constants that correct for the *J*- and *K*- dependence of the Coriolis zeta parameter, respectively. The first fit had the unusual feature that the  $q^+$  *l*-type doubling constant for  $v_6$  was not well determined, but it was necessary to include higher order  $q_I$  and  $q_K$  corrections that account for the *J*- and *K*- dependence of the *l*-type doubling.

In this work, we have used CF<sub>3</sub>I as a test molecule for evaluation of a newly constructed chirped-pulse Fourier-transform microwave (CP-FTMW) spectrometer, <sup>19,20</sup> operating in the 2–8

GHz region. We found expansion conditions that favored the generation of CF<sub>3</sub>I in the excited  $\nu_6$  vibrational state, enabling measurements of the J=1-0 and J=2-1 spectral regions. The spectrum exhibits structure due to the large nuclear quadrupole coupling constant arising from the  $^{127}I$  nucleus as well as l-type doubling that arises from the doubly degenerate vibration. Our measured frequencies agree poorly with the predictions of spectroscopic constants for the interacting  $\nu_6$  and  $\nu_3$  levels reported from the millimeter-wave work of Walters and Whiffen<sup>15</sup> and the IR study of Willaert *et al.*,  $^{18}$  which motivated us to re-evaluate the fit model. We report the results of fitting our updated model to a combined dataset that includes all microwave, millimeter-wave, and IR transition frequencies reported here and in Refs. 15,17,18. Our fit model is guided by the results of *ab initio* anharmonic force field calculations.

#### **Experimental**

A schematic diagram of the newly constructed microwave spectrometer is shown in Fig. 1. The design is based on the compact 2-8 GHz spectrometer reported by Neill et al.<sup>21</sup> A chirped excitation pulse is produced by an arbitrary waveform generator (AWG, Tektronix 710B). The frequency and bandwidth of the pulse are multiplied by four using an active quadrupler that was constructed from surplus parts. The resulting chirped pulse is amplified by a 10 W solid state amplifier (RF-Lambda, RFLUPA01G09GA) and coupled into free space by a high gain antenna (ATM 250-441EM-NF). A single-pole single-throw (SPST, KDI SW-2018AC) switch is used on the output of the amplifier to reduce the noise floor during signal collection. The free induction decay (FID) emitted by the sample is collected by a matched antenna and sent through a low-noise amplifier (LNA, RF-Lambda RLNA02G08G30D). The LNA is protected from the excitation pulse by a limiter (CAES ACLM-4601) and a SPST switch (KDI SW-2018AC). Finally, the FID is down-converted in a mixer (Watkins Johnson M93C) using a 4 GHz phase-locked oscillator (Lotus Systems) as the LO, and the FID is averaged in the time domain on a 2.5 GHz oscilloscope (Teledyne Lecroy WavePro 254HD) operating at a 20 GS/s sampling rate. A 10 MHz rubidium oscillator (SRS FS725) is used to provide phase stability and frequency accuracy. We are currently in the process of upgrading the oscilloscope to the full bandwidth of 8 GHz, and we plan to make additional modifications to improve the spectrometer's sensitivity.

We found that population of the excited  $\nu_6$  state was favored by expansion of CF<sub>3</sub>I in Ar with mixing ratios in the range of 1–10%. The  $\nu_6$  lines were absent when N<sub>2</sub> was used as the seed gas, and they were also not observed in a previously reported spectrum<sup>22</sup> using Ne. Spectra of CF<sub>3</sub>I were acquired for a 10% CF<sub>3</sub>I/Ar mixture. CF<sub>3</sub>I (99% purity) was obtained from Sigma Aldrich

and used without further purification. The sample was placed in a stainless-steel reservoir at room temperature and was expanded into a four-way cross vacuum chamber through a pulsed nozzle (Ideal Vacuum Pulse Valve, P1010774) at a backing pressure of 1 bar and a repetition rate of 20 Hz. The vacuum chamber is evacuated by a diffusion pump (Varian VHS-6) to a baseline pressure of  $\sim 10^{-7}$  mbar.

#### **Calculations**

The minimum energy geometry and force field of CF<sub>3</sub>I was calculated using the CFOUR package.<sup>23</sup> Calculations were performed at the MP2, CCSD, and CCSD(T) levels of theory with a series of Pople basis sets extending up to 6-311G\*\*.<sup>24</sup> At the CCSD(T) level of theory, only the harmonic force field was calculated. At the MP2 and CCSD levels of theory, the cubic anharmonic force field was calculated, allowing calculations of fundamental vibrational frequencies and vibration-rotation constants. At this level of theory, the vibrational frequencies and the absolute rotational constants are not expected to be spectroscopically accurate. However, the vibration-rotation constants (α values), can be significantly more reliable than the absolute rotational constants. Quartic centrifugal distortion constants and Coriolis zeta constants can be calculated quite accurately from the harmonic force field and can be meaningfully compared with (deperturbed) experimental values. The calculated rotational constants, vibration-rotation constants, and fundamental frequencies are given in Table 1. Experimental values are shown for comparison. Calculated geometries are given in Table S1, and calculated centrifugal distortion constants and Coriolis zeta constants are given in Table S2 of the SI.

#### **Results**

Figure 2 shows an overview of the 2–8 GHz spectrum of  $CF_3I$ . The spectrum was acquired at a resolution of 50 kHz with a total of 600000 averages for both signal and background with total acquisition time of around 17 hours. In addition to the strong lines from the  $CF_3I$  ground state, we also observe lines from the  $^{13}CF_3I$  isotopologue (Fig. 2 inset) in natural abundance and arising from the vibrationally excited  $\nu_6$  level of  $^{12}CF_3I$ . The simulated frequencies and intensities were calculated using the SPCAT/SPFIT suite<sup>25</sup> and are shown for comparison in Fig. 2. The frequencies of  $^{13}CF_3I$  lines and vibrational satellites have not been previously reported in this frequency range and are listed in Table 2.

The most recently reported spectroscopic constants for ground-state <sup>12</sup>CF<sub>3</sub>I<sup>14</sup> and <sup>13</sup>CF<sub>3</sub>I<sup>15</sup> were in good agreement with our observation, so we made no attempts to fit these datasets. However, the predicted line positions for the  $v_6$  vibrational satellites deviated significantly from the prediction calculated using the parameters of Walters and Whiffen<sup>15</sup> and from the prediction calculated using the parameters of Willaert et al. 18 (Fig. 3A). The splitting between the l-type doubled k = 1 satellites that arise from transitions between  $A_1$  and  $A_2$  rovibrational species exhibited particularly poor agreement. We therefore re-evaluated the spectroscopic constants using two different models. In the first model, we considered  $v_6$  as an isolated state, and we fit a combined dataset consisting of our microwave measurements, the millimeter-wave measurements of Walters and Whiffen, 26 and the *l*-type doubling transitions of Gerke and Harder. 17 We found that the introduction of the  $eQq\eta$  parameter allowed our low-J data to be fit adequately. This parameter<sup>27</sup> can be thought of as a vibrationally induced asymmetry in the  $\chi_{bb}$  and  $\chi_{cc}$  components of the nuclear quadrupole coupling tensor, which gives rise to  $\Delta K = \pm 2$ ,  $\Delta l = \pm 2$  matrix elements and allows the effective *l*-type doubling to depend rather strongly on the nuclear spin state. It was also necessary to include the  $C_6$  spin-rotation interaction parameter to obtain a proper fit to the *l*type doubling transitions. The fit results are shown in Table 3. Most of the parameters obtained were similar to those obtained by Walters and Whiffen. The  $q_1$ ,  $eQq\eta$ , and  $C_6$  parameters were similar to those reported by Gerke and Harder. The overall rms error was 0.083 MHz. However, it is important to consider that the various sources of data spanned a large range of measurement accuracies, so it was important to weight each observed frequency according to the stated measurement uncertainty. A summary of the rms fit error obtained from each dataset is given at the bottom of Table 3. Note that the rms fit errors are in quite reasonable agreement with the respective measurement uncertainties.

We performed a second fit that explicitly accounts for the Coriolis interaction between the  $v_3$  and  $v_6$  levels. We fit a combined dataset of 3593 frequencies, which included all the  $v_6$  microwave transitions used in the first fit as well as 137  $v_3$  millimeter wave transitions from Ref. <sup>26</sup> and 3053  $v_3$  fundamental IR transitions from Ref. <sup>18</sup>. It is challenging to model such an interaction given that the precise  $v_6$  fundamental frequency is unknown. Even a handful of rotationally resolved  $v_6$  fundamental IR transitions would enable significantly more constraints to be placed on the fit model. Not only would such data provide the  $v_3 - v_6$  energetic separation, the perpendicular  $v_6$  fundamental transition would also provide information about the  $A_6$  rotational constant and the  $D_k$  centrifugal distortion constant, both of which are correlated to other fitting parameters. For example, in the most recent attempt by Willaert *et al.* <sup>18</sup> to fit the interaction, two

different fits were attempted using different values of the  $v_6$  fundamental frequency (see Table 4). With either choice, the authors were able to achieve very good agreement with the available data. However, the two fits yielded radically different values of the  $A_6$  rotational constant, which is not well determined by the available microwave data. Our approach was to obtain the most physically reasonable fit model by using the results of *ab initio* force field calculations to constrain as many of the poorly determined parameters as possible.

Unfortunately, calculations performed within the Born-Oppenheimer approximation typically result in  $\pm$  10 cm<sup>-1</sup> errors in vibrational frequencies so that the  $\nu_6$  frequency cannot be meaningfully constrained by the available theory. However, centrifugal distortion constants and Coriolis zeta parameters obtained from *ab initio* force fields can be quite reliable for molecules of this size. It can be more challenging to compare experimentally derived vibration-rotation constants with those obtained by applying perturbation using the cubic force field parameters, <sup>28</sup> particularly for higher frequency vibrations that can participate in complicated interactions with lower frequency modes. However, for the lowest-frequency vibrational states considered here, the interaction is isolated, and its analysis can be guided by *ab initio* vibration-rotation constants.

The best-fit parameters of our model are given in Table 4. Note that the reported uncertainties reflect only the statistical uncertainty in the fit and do not include systematic errors due to correlation or due to inadequacies in the model. The ground state parameters were constrained to literature values obtained from microwave spectroscopy, with the exception of the  $D_K^0$  centrifugal distortion parameter, which is not well determined by spectroscopy, but which affects the fit of the Coriolis interaction. The  $D_K$  parameter for all levels was therefore constrained to the ab initio value. For the  $v_6$  level, the  $A_6$  rotational constant was constrained to the ab initio value,  $\mathcal{D}_{J}^{6}$  was constrained to the ground state value, and the  $eQq_{6}$  nuclear quadrupole coupling constant and  $C_6$  spin-rotation interaction constant were constrained to the literature values of Refs. 15 and <sup>17</sup>, respectively. The other parameters, including the  $B_6$  rotational constant and the  $v_6$ fundamental frequency were floated. In order to fit the high-resolution l-type doubling transitions 17 adequately, it was necessary to include a  $q_l$  centrifugal distortion correction to the l-type doubling constant. The  $eQq_3$  constant for the  $v_3$  level was constrained to the literature value. 15 The  $v_3$ - $v_6$ b-axis Coriolis matrix element was constrained using the ab initio  $\zeta_{36}^{(b)}$  value. We attempted to include a  $q_K$  centrifugal distortion correction to the l-type doubling constant as well as higher order  $C_x^I$  and  $C_x^K$  centrifugal distortion corrections to the Coriolis interaction as was necessary to achieve the fits reported in Ref. 18, but none of these higher order parameters improved the quality of the fit. We use the definitions of  $C_0$  and  $C_6$  spin-rotation parameters given in Refs. 14 and 15, respectively. The  $eQq\eta$  parameter is defined in the same way as the  $\chi_6$  parameter given in Ref. <sup>17</sup>. The definitions of the  $C_x^I$  and  $C_x^K$  parameters shown in Table 4 are given in Ref. <sup>18</sup>.

The fit errors are summarized in Table 5. The errors were somewhat larger than those obtained from the effective, isolated  $v_6$  fit (Table 3). However, the low-J transitions reported here, the millimeter-wave transitions of Ref. 15, and the  $v_3$  IR data<sup>18</sup> are all fitted with rms errors that are smaller than or similar to the reported measurement uncertainties. The l-type doubling transitions reported by Gerke and Harder<sup>17</sup> were recorded with high frequency resolution (~1.8 kHz measurement error), but are fitted with an rms error of 7.1 kHz, indicating that the model is not capable of reproducing all observations perfectly. (The rms error for this data set obtained in the fit by Willaert  $et\ al.^{18}$  was 8.4 kHz.) It was possible to achieve a better fit by floating the  $D_J^6$  parameter, but this led to a value that was inconsistent with the force field prediction. We believe the model parameters are more physically meaningful with the constraint in place.

A list of residuals (Obs – Calc) to our new observations is printed in Table 2b. A full list of the observed transitions and their fit residuals are given in the Supplementary Information. Figure 3b illustrates the quality of the fit to the low-J l-type doubled  $\nu_6$  vibrational sattelites reported here. The quality of the fit the  $\nu_3$  IR spectrum<sup>18</sup> is illustrated in Fig. 4.

#### **Discussion**

We considered the physical reasonableness of our model parameters. The  $D_{JK}^6$ ,  $D_J^3$ , and  $D_{JK}^3$  parameters were floated but differed from their ground state values by only 17 Hz, 3.6 Hz, and 9 Hz, respectively, indicating that they are not strongly perturbed by the Coriolis interaction. A comparison of other parameters to predictions of the *ab initio* force field is made in Table 6. The *ab initio* rotation-vibration constants listed in the table include the quadratic and anharmonic correction terms of Ref. <sup>28</sup>, but do not include the Coriolis correction since that interaction is treated explicitly in the model. In particular, note that our  $\alpha_6^{(A)}$  parameter was constrained to match the MP2 6-311G\*\* value, whereas the corresponding values obtained by Walters and Whiffen<sup>15</sup> and the two Willaert models<sup>18</sup> differ from the *ab initio* value by 7.7 MHz, 8.4 MHz, and  $\alpha_3^{(B)}$  vibration-rotation constants differ from the MP2 6-311G\*\* prediction by only 24 kHz and 234 kHz, respectively. The  $\alpha_3^{(B)}$  parameters in Willaert's Calc. 3<sup>18</sup> differs from the ab initio value by at least 1.5 MHz. Our  $\alpha_6^{(B)}$  parameter differs from the *ab initio* value by 520 kHz, which may indicate that the  $B_6$  rotational constant is still slightly perturbed by the interaction. In our fit, the  $\zeta_{36}^{(b)}$  parameter

was constrained to the MP2 value. In Willaert's Calc. 3, the discrepancy with the *ab initio*  $\zeta_{36}^{(b)}$  parameter is significant, which may indicate that this model is based on unreasonable assumptions.

Our analysis of the rotational structure favors a high  $v_6$  value of 267.28 cm<sup>-1</sup>, similar to the value reported by Walters and Whiffen<sup>15</sup> and the value obtained in Willaert's Calc. 2 model.<sup>18</sup> This value is consistent with a  $v_3 - v_6$  frequency difference of 19.0 cm<sup>-1</sup>. This value disagrees with the value  $v_6 = 261.5 \pm 1.5 \text{ cm}^{-1}$ , derived from careful consideration of the vibrational level structure.  $^{16}$  In order to address this discrepancy, we performed a second fit in which  $\nu_6$  was constrained to 261.5 cm<sup>-1</sup>. With this constraint, it was possible to fit the microwave (this work and Ref. 17) and millimeter-wave<sup>15</sup> observations with rms errors of 22 kHz and 350 kHz, respectively, and the high-resolution  $\nu_3$  IR data<sup>18</sup> with an rms error of  $2.8 \times 10^{-4}$  cm<sup>-1</sup>. This fit required the use of high-order  $C_x^I$  and  $C_x^K$  corrections to the Coriolis interaction matrix elements, similar to the ones obtained in the Calc. 3 model of Willaert et al. 18 Similar to the Calc. 3 model, the fit leads to a high value of  $A_6 = 5785.58 \text{ cm}^{-1}$ , and it leads to a  $\zeta_{36}^{(b)}$  value of 0.5570, which is 40% higher than the value obtained from the harmonic force field. For these reasons, the perturbed rotational structure appears to be more naturally consistent with the high  $\nu_6$  value. However, the fact that a good fit can be achieved with both  $\nu_6$  values clearly demonstrates correlation among the model parameters. Indirect determination of the  $v_6$  frequency by our fitting model is inconclusive, and we cannot rule out the lower value that is favored by analysis of the vibrational level structure.

#### Conclusion

We have evaluated the performance of a newly constructed CP-FTMW spectrometer, demonstrating that we can readily observe vibrational satellites and  $^{13}$ C peaks in natural abundance. We have re-evaluated the spectroscopic constants for the interacting  $\nu_3$  and  $\nu_6$  vibrational levels of CF<sub>3</sub>I, and we have obtained an updated fit to the complete set of frequencies reported here and in the literature. Although our analysis favors a high  $\nu_6$  value of 267.28 cm<sup>-1</sup>, the evidence is insufficient to rule out the lower value of  $\nu_6 = 261.5$  cm<sup>-1</sup>, obtained from evaluation of the vibrational level structure.

#### **Acknowledgments**

This material is based upon work supported by the National Science Foundation under Grant No. 2340303. G.B.P. is grateful to Bob Field for generously donating some of the equipment

used to build the preliminary Chirped Pulse spectrometer described in this work. The authors thank Agnès Perrin and Laurent Manceron for graciously providing us with a list of their observed frequencies for the  $\nu_3$  fundamental transition.

#### References

- 1. J. Zhang, D. J. Wuebbles, D. E. Kinnison, A. Saiz-Lopez, "Revising the Ozone Depletion Potentials Metric for Short-Lived Chemicals Such as CF<sub>3</sub>I and CH<sub>3</sub>I" *Journal of Geophysical Research:* Atmospheres 125, e2020JD032414 (2020), https://doi.org/10.1029/2020JD032414.
- 2. Y. Kobayashi, I. Kumadaki, "Trifluoromethylation of aromatic compounds" *Tetrahedron Lett.* **10**, 4095-4096 (1969), <a href="https://doi.org/10.1016/S0040-4039(01)88624-X">https://doi.org/10.1016/S0040-4039(01)88624-X</a>.
- 3. Y. He, J. Pochert, M. Quack, R. Ranz, G. Seyfang, "Dynamics of unimolecular reactions induced by monochromatic IR radiation: experiment and theory for  $C_nF_mH_kI \rightarrow C_nF_mH_k+I$  probed with hyperfine-, doppler- and uncertainty-limited time resolution of iodine-atom IR absorption " *Faraday Discuss.* **102**, 275-300 (1995), https://doi.org/10.1039/FD9950200275.
- 4. W. F. Edgell, C. E. May, "Raman and Infrared Spectra of CF<sub>3</sub>Br and CF<sub>3</sub>I" *J. Chem. Phys.* **22**, 1808-1813 (1954), <a href="https://doi.org/10.1063/1.1739925">https://doi.org/10.1063/1.1739925</a>.
- 5. R. J. H. Clark, O. H. Ellestad, "The vapour phase Raman spectra, Raman band contour analyses, Coriolis coupling constants, and *e*-species force constants for the molecules HCF<sub>3</sub>, ClCF<sub>3</sub>, BrCF<sub>3</sub>, and ICF<sub>3</sub>" *Mol. Phys.* **30**, 1899-1911 (1975), https://doi.org/10.1080/00268977500103371.
- 6. W. B. Person, S. K. Rudys, J. H. Newton, "Absolute integrated infrared absorption intensities of trichlorofluoromethane and trifluoroiodomethane fundamentals in the gas phase. Intensity sum rule" *J. Phys. Chem.* **79**, 2525-2531 (1975), https://doi.org/10.1021/j100590a016.
- 7. W. Fuss, "Fundamental and overtone infrared spectra of  $CF_3$ I" Spectrochimica Acta Part A: Molecular Spectroscopy **38**, 829-840 (1982), <a href="https://doi.org/10.1016/0584-8539(82)80102-5">https://doi.org/10.1016/0584-8539(82)80102-5</a>.
- 8. F. Kohler, H. Jones, H. D. Rudolph, "Laser-microwave double-resonance spectroscopy in CF<sub>3</sub>I with four CO<sub>2</sub>-laser lines" *J. Mol. Spectrosc.* **80**, 56-70 (1980), https://doi.org/10.1016/0022-2852(80)90270-2.
- 9. J. G. McLaughlin, M. Poliakoff, J. G. Smith, S. Walters, "Direct observation of the v<sub>6</sub> band in the IR spectrum of CF<sub>3</sub>I dissolved in liquid xenon" *J. Mol. Struct.* **102**, 289-293 (1983), https://doi.org/10.1016/0022-2860(83)85066-2.
- J. Sheridan, W. Gordy, "The Microwave Spectra and Molecular Structures of Trifluoromethyl Bromide, Iodide, and Cyanide" J. Chem. Phys. 20, 591-595 (1952), https://doi.org/10.1063/1.1700499.
- 11. F. Sterzer, "J =  $0 \rightarrow 1$  Rotational Transition of Trifluoroiodomethane" J. Chem. Phys. 22, 2094-2094 (1954), https://doi.org/10.1063/1.1740013.
- 12. H. Jones, F. Kohler, "Infrared-microwave double resonance in CF<sub>3</sub>I; Microwave spectroscopy in emission and absorption" *J. Mol. Spectrosc.* **58**, 125-141 (1975), https://doi.org/10.1016/0022-2852(75)90161-7.

- 13. A. P. Cox, G. Duxbury, J. A. Hardy, Y. Kawashima, "Microwave spectra of CF<sub>3</sub>Br and CF<sub>3</sub>I. Structures and dipole moments" *Journal of the Chemical Society, Faraday Transactions 2: Molecular and Chemical Physics* **76**, 339-350 (1980), <a href="https://doi.org/10.1039/F29807600339">https://doi.org/10.1039/F29807600339</a>.
- 14. S. L. Stephens, N. R. Walker, "Determination of nuclear spin—rotation coupling constants in CF<sub>3</sub>I by chirped-pulse Fourier-transform microwave spectroscopy" *J. Mol. Spectrosc.* **263**, 27-33 (2010), <a href="https://doi.org/10.1016/j.jms.2010.06.007">https://doi.org/10.1016/j.jms.2010.06.007</a>.
- 15. S. W. Walters, D. H. Whiffen, "Rotational spectrum of trifluoroidomethane" *Journal of the Chemical Society, Faraday Transactions 2: Molecular and Chemical Physics* **79**, 941-949 (1983), https://doi.org/10.1039/F29837900941.
- 16. H. Bürger, K. Burczyk, H. Hollenstein, M. Quack, "High resolution FTIR spectra of  $^{12}\text{CF}_3\text{I}$ ,  $^{13}\text{CF}_3\text{I}$  and  $^{12}\text{CF}_3^{79}\text{Br}$  near 1050 cm<sup>-1</sup> and 550 cm<sup>-1</sup>" *Mol. Phys.* **55**, 255-275 (1985), https://doi.org/10.1080/00268978500101311.
- 17. C. Gerke, H. Harder, "Direct *l*-type doubling transitions in the  $v_6$  = 1 vibrational state of CF<sub>3</sub>Br and CF<sub>3</sub>I: *l*-type resonance effects on the spin-rotation coupling" *Chem. Phys. Lett.* **255**, 287-294 (1996), https://doi.org/10.1016/0009-2614(96)00399-5.
- 18. F. Willaert, P. Roy, L. Manceron, A. Perrin, F. Kwabia-Tchana, D. Appadoo, D. McNaughton, C. Medcraft, J. Demaison, "High resolution investigation of the v<sub>3</sub> band of trifluoromethyliodide (CF<sub>3</sub>I)" *J. Mol. Spectrosc.* **315**, 16-23 (2015), https://doi.org/10.1016/j.jms.2014.12.021.
- 19. G. G. Brown, B. C. Dian, K. O. Douglass, S. M. Geyer, S. T. Shipman, B. H. Pate, "A broadband Fourier transform microwave spectrometer based on chirped pulse excitation" *Rev. Sci. Instrum.* **79**, 053103 (2008), <a href="http://doi.org/10.1063/1.2919120">http://doi.org/10.1063/1.2919120</a>.
- 20. G. B. Park, R. W. Field, "Perspective: The first ten years of broadband chirped pulse Fourier transform microwave spectroscopy" *J. Chem. Phys.* **144**, (2016), http://doi.org/10.1063/1.4952762.
- 21. J. L. Neill, S. T. Shipman, L. Alvarez-Valtierra, A. Lesarri, Z. Kisiel, B. H. Pate, "Rotational spectroscopy of iodobenzene and iodobenzene—neon with a direct digital 2–8 GHz chirped-pulse Fourier transform microwave spectrometer" *J. Mol. Spectrosc.* **269**, 21-29 (2011), https://doi.org/10.1016/j.jms.2011.04.016.
- D. Schmitz, V. Alvin Shubert, T. Betz, M. Schnell, "Multi-resonance effects within a single chirp in broadband rotational spectroscopy: The rapid adiabatic passage regime for benzonitrile" *J. Mol. Spectrosc.* 280, 77-84 (2012), https://doi.org/10.1016/j.jms.2012.08.001.
- 23. CFOUR, a quantum chemical program package written by J.F. Stanton, J. Gauss, L. Cheng, M.E. Harding, D.A. Matthews, P.G. Szalay with contributions from A. Asthana, A.A. Auer, R.J. Bartlett, U. Benedikt, C. Berger, D.E. Bernholdt, S. Blaschke, Y.J. Bomble, S. Burger, O. Christiansen, D. Datta, F. Engel, R. Faber, J. Greiner, M. Heckert, O. Heun, M. Hilgenberg, C. Huber, T.-C. Jagau, D. Jonsson, J. Jusélius, T. Kirsch, M.-P. Kitsaras, K. Klein, G.M. Kopper, W.J. Lauderdale, F. Lipparini, J. Liu, T. Metzroth, L.A. Mück, T. Nottoli, D.P. O'Neill, J. Oswald, D.R. Price, E. Prochnow, C. Puzzarini, K. Ruud, F. Schiffmann, W. Schwalbach, C. Simmons, S. Stopkowicz, A. Tajti, T. Uhlířová, J. Vázquez, F. Wang, J.D. Watts, P. Yergün, C. Zhang, X. Zheng and the integral packages MOLECULE (J. Almlöf and P.R. Taylor), PROPS (P.R. Taylor), ABACUS (T. Helgaker, H.J. Aa. Jensen, P. Jørgensen, and J. Olsen), and ECP

- routines by A. V. Mitin and C. van Wüllen. For the current version, see <a href="http://www.cfour.de">http://www.cfour.de</a>.
- 24. R. Krishnan, J. S. Binkley, R. Seeger, J. A. Pople, "Self-consistent molecular orbital methods. XX. A basis set for correlated wave functions" *J. Chem. Phys.* **72**, 650-654 (1980), https://doi.org/10.1063/1.438955.
- 25. H. M. Pickett, "The fitting and prediction of vibration-rotation spectra with spin interactions" *J. Mol. Spectrosc.* **148**, 371-377 (1991), <a href="https://doi.org/10.1016/0022-2852(91)90393-0">https://doi.org/10.1016/0022-2852(91)90393-0</a>.
- 26. S. W. Walters, D. H. Whiffen, Supplementary Publication No. SUP 23561, The British Library, (1983).
- 27. G. Tarrago, S. Maes, "Influence de la vibration sur la structure hyperfine des niveaux de rotation des molécules à symétrie ternaire" *Comptes rendus de l'Académie des Sciences Series II* **266**, 699 (1968).
- 28. I. M. Mills, in *Molecular Spectroscopy: Modern Research*, ed. by K. N. Rao, C. W. Mathews, Academic Press, New York, **1972**, pp. 115.
- 29. V. Typke, M. Dakkouri, H. Onerhammer, "On the molecular structure of X-CF $_3$  molecules (X = Cl, Br, I)" *J. Mol. Struct.* **44**, 85-96 (1978), <a href="https://doi.org/10.1016/0022-2860(78)85008-X">https://doi.org/10.1016/0022-2860(78)85008-X</a>.
- 30. Y. He, H. Hollenstein, M. Quack, E. Richard, M. Snels, H. Bürger, "High resolution analysis of the complex symmetric CF<sub>3</sub> stretching chromophore absorption in CF<sub>3</sub>I" *J. Chem. Phys.* **116**, 974-983 (2002), https://doi.org/10.1063/1.1370948.
- 31. Y. Matsumoto, M. Takami, P. A. Hackett, "High-resolution infrared absorption spectroscopy of the  $CF_3l$   $v_2$  band" *J. Mol. Spectrosc.* **118**, 310-312 (1986), https://doi.org/10.1016/0022-2852(86)90244-4.
- 32. P. B. Davies, N. A. Martin, M. D. Nunes, "Diode laser spectroscopy of the 4<sup>1</sup><sub>0</sub> band of <sup>12</sup>CF<sub>3</sub>I and <sup>13</sup>CF<sub>3</sub>I in a supersonic jet" *Spectrochimica Acta Part A: Molecular Spectroscopy* **45**, 293-298 (1989), https://doi.org/10.1016/0584-8539(89)80136-9.

#### **Tables**

**Table 1.** Ground-state rotational constants, vibration-rotation constants, and fundamental vibrational frequencies of  $^{12}\text{CF}_3\text{I}$ , obtained from *ab initio* anharmonic force field calculations are compared with experimental values. For the experimental  $\nu_6$  fundamental frequency, we include the value obtained in this work from a model of the  $\nu_3$ - $\nu_6$  Coriolis interaction as well as the value recommended in Ref.  $^{16}$ , which is based on a comprehensive vibrational analysis, including the energetic positions of overtone and combination levels.

		HF			MP2			CCSD		
Param.	3-21G	6-311G	6-311G**	3-21G	6-311G	6-311G**	3-21G	6-311G	6-311G**	Expt.
$A_0/\mathrm{MHz}$	5607.00	5546.54	5911.00	5365.13	5215.47	5692.53	5382.05	5254.75	5722.32	5759.01a
$B_0/\mathrm{MHz}$	1470.47	1493.24	1524.95	1428.16	1452.68	1497.95	1423.70	1449.31	1494.97	1523.28287(2)b
$lpha_6^{(A)}$ /MHz	-7.46	-6.88	-7.85	-7.17	-6.16	-7.72	-7.36	-6.46	-7.86	
$\alpha_6^{(B)}$ /MHz	0.764	0.696	0.675	1.033	0.782	0.842	1.105	0.862	0.853	1.36254(21) <sup>c</sup>
$\alpha_3^{(A)}$ /MHz	0.357	0.399	0.246	0.522	0.531	0.402	0.525	0.489	0.375	0.4254(25) <sup>c</sup>
$lpha_3^{(B)}$ /MHz	2.58	2.38	2.76	3.29	2.66	3.35	3.40	2.77	3.30	3.5822(3) <sup>c</sup>
$ u_1$	1169.50	1142.05	1182.10	1061.05	1011.13	1072.40				1076.0551(1) <sup>d</sup>
$\nu_2$	748.33	733.51	814.88	689.90	655.77	748.28				743.36912(12)e
$\nu_3$	296.90	306.14	309.21	269.78	284.94	284.58				286.297298(32) <sup>c</sup>
$ u_4$	1361.69	1229.61	1337.79	1242.26	1068.49	1214.01				1187.62771(5)f
$ u_5$	539.93	525.16	577.91	501.41	467.79	538.06				539.830(7)g
$\nu_6$	277.81	283.10	296.59	259.38	263.04	276.20				267.28155(33) <sup>c</sup> 261.5(15) <sup>g</sup>

aRef. 29.

<sup>&</sup>lt;sup>b</sup>Ref. 14.

<sup>&</sup>lt;sup>c</sup>This work.

dRef. 30.

eRef. 31.

fRef. 32.

<sup>&</sup>lt;sup>g</sup>Ref. 16.

**Table 2a.** <sup>13</sup>CF<sub>3</sub>I lines. The Obs – Calc residuals are obtained using the parameters of Ref. 15. Frequencies are given in units of MHz.

J'	K'	F'	$J^{\prime\prime}$	<i>K''</i>	$F^{\prime\prime}$	Obs Freq	Obs — Calc
2	0	3.5	1	0	3.5	5700.838	-0.118
2	1	3.5	1	1	2.5	5782.983	-0.079
2	0	2.5	1	0	3.5	5829.291	-0.051
2	0	4.5	1	0	3.5	6114.379	0.007
2	0	3.5	1	0	2.5	6148.549	0.048
2	1	4.5	1	1	3.5	6204.338	0.081

**Table 2b.** Observed transitions in the  $v_6 = 1$ ,  $l = \pm 1$  vibrational state. The Obs – Calc residuals are from the fit parameters given in Table 4. Frequencies are given in units of MHz.

											Obs
J'	K'	l'	F'	sym'	$J^{\prime\prime}$	$K^{\prime\prime}$	$l^{\prime\prime}$	$F^{\prime\prime}$	sym''	Obs Freq	— Calc
1	0		3.5	Е	0	0		2.5	Е	3157.4967	0.0348
1	0		1.5	E	0	0		1.5	E	3357.7249	-0.0421
2	0		2.5	E	1	0		1.5	E	5645.9870	-0.0055
2	0		3.5	E	1	0		3.5	E	5718.3919	0.0033
2	1	1	3.5	$\mathbf{A}_1$	1	1	1	2.5	$A_2$	5794.7035	0.0217
2	1	-1	3.5	E	1	1	-1	2.5	E	5800.5376	0.0068
2	1	1	3.5	$\mathbf{A}_2$	1	1	1	2.5	$A_1$	5806.1112	0.0229
2	1	1	2.5	$\mathbf{A}_{1}$	1	1	1	2.5	$A_2$	5841.2197	0.0083
2	1	-1	2.5	E	1	1	-1	2.5	E	5846.7933	-0.0388
2	1	1	2.5	$\mathbf{A}_2$	1	1	1	2.5	$A_1$	5852.1586	-0.0072
2	0		1.5	E	1	0		1.5	E	5936.4921	-0.0070
2	1	1	1.5	$\mathbf{A}_1$	1	1	1	2.5	$A_2$	6010.8764	-0.0355
2	1	-1	1.5	E	1	1	-1	2.5	E	6015.8770	-0.0277
2	1	-1	3.5	E	1	1	-1	3.5	E	6032.8583	0.0147
2	0		4.5	E	1	0		3.5	E	6131.8811	0.0432
2	0		3.5	E	1	0		2.5	E	6165.9999	0.0227
2	0		0.5	E	1	0		1.5	E	6212.8287	0.0106
2	1	1	4.5	$\mathbf{A}_1$	1	1	1	3.5	$A_2$	6215.9020	0.0248
2	1	-1	4.5	E	1	1	-1	3.5	E	6221.8402	0.0522
2	1	1	4.5	$\mathbf{A}_2$	1	1	1	3.5	$A_1$	6227.4138	-0.0041
2	0		2.5	E	1	0		2.5	E	6293.8284	-0.0578
2	1	1	1.5	$\mathbf{A}_1$	1	1	1	1.5	$A_2$	6343.8867	0.0099
2	1	-1	1.5	E	1	1	-1	1.5	E	6350.1896	-0.0194
2	1	1	1.5	$\mathbf{A}_2$	1	1	1	1.5	$A_1$	6356.2320	-0.0264
2	1	1	0.5	$\mathbf{A}_1$	1	1	1	1.5	$\mathbf{A}_2$	6463.1204	-0.0091
2	1	-1	0.5	E	1	1	-1	1.5	E	6468.7982	-0.0470
2	1	1	0.5	$\mathbf{A}_2$	1	1	1	1.5	$\mathbf{A}_1$	6474.2676	-0.0208

**Table 3**: Fit parameters for  $v_6$  data, treating  $v_6$  as an isolated state. Standard errors in units of the final printed digit are given in parentheses.

Parameter	This work	Ref. 15	Ref. <sup>17</sup>
A / MHz	5760 <sup>a</sup>	5760	
B/MHz	1520.628065(72)	1520.6281(1)	
$D_J$ / kHz	0.16181(14)	0.16185(8)	
$D_{JK}$ / kHz	1.1929(15)	1.1934(10)	
$H_{JKK}$ / Hz	-0.07137(110)	-0.070(2)	
$A\zeta$ / MHz	798.3(38)	787.5(39)	
$\eta_J$ / kHz	-18.023(21)	-18.005(6)	
$\eta_{JK}/\mathrm{Hz}$	-1.618(41)	-1.65(7)	
$q^+$ / MHz	-2.93549738(37)	-2.9360(5)	2.93549750(72)
$q_J$ / Hz	4.97256(16)	2.9(4)	-4.97260(32)
eQq / MHz	-2144.58a	-2144.58(12)	
$eQq\eta$ / MHz	-9.0279(16)		-9.0278(32)
$C_6$ / $Hz$	-81.1(16)		-84.7(31)

Dataset	Description	No. of Transitions	Ave. Msmt Error	rms Fit Error
Ref. 15	mm-wave, $J = 11-46$	304	240 kHz	128 kHz
Ref. 17	<i>l</i> -type doubling transitions	72	1.8 kHz	2.2 kHz
This work	J = 0-2	27	50 kHz	28 kHz

<sup>a</sup>Constrained to the value of Ref. 15.

**Table 4**: Parameters for the global fit of the interacting  $v_3$ - $v_6$  levels.

Parameters	This work	Ref. 15	Ref. 18, Calc. 2	Ref. 18, Calc. 3
		ground state		
$A_0$ / MHz	5759.01*a	5760*	5759.01*	5759.01*
$B_0 / \mathrm{MHz}$	1523.28267*b	1523.28267(9)	1523.28267*	1523.28267*
$D_J^0$ / kHz	0.16462* b	0.16462(2)	0.16462*	0.16462*
$D_{JK}^0 /  m kHz$	0.9925*b	0.9925(4)	0.9925*	0.9925*
$D_K^0$ / kHz	0.31937*c		0.294*	0.294*
$eQq_0$ / MHz	-2145.207*b	-2145.207(3)		
$C_0$ / $kHz$	6.88*d	4.7(6)		
		$v_6 = 1$		
ν <sub>6</sub> / cm <sup>-1</sup>	267.28155(33)	267.3*	267.65*	261.5*
$A_6$ / MHz	5766.7266*c	5760*	5758.58175*	5782.4847(24)
$B_6$ / MHz	1521.92013(21)	1522.02	1522.07788(10)	1522.5576(31)
$D_J^6$ / kHz	0.16462*e	0.1627	0.16462*	0.16462*
$D_{JK}^6$ / kHz	0.9753(11)	0.9916	1.02069(330)	1.02228(150)
$D_K^6/\mathrm{kHz}$	0.31937*c,e		0.294*	0.294*
$A_6\zeta_{66}^{(a)}$ / MHz	793.80(50)	787.5*	787.5*	787.5*
$\eta_J^6$ / kHz	-2.414(25)	-1.263		
q <sup>+</sup> / MHz	-0.320319(46)	-0.1269	0	0.9597(60)
$q_J$ / Hz	2.5523(14)		-1.295(80)	-1.232(56)
$q_K$ / MHz			0.214(28)	
$eQq_6$ / MHz	-2144.58*b	-2144.58(12)		
$eQq\eta$ / $MHz$	-9.0212(21)			
$C_6$ / $Hz$	-84.7*f			
		$v_3 = 1$		
$\nu_3$ / cm $^{-1}$	286.297298(32)		286.29712(3)	286.29713(5)
$A_3$ / MHz	5758.58458(25)	5760	5758.58175(320)	5758.5799(48)
$B_3 / \mathrm{MHz}$	1519.70047(27)	1519.51	1519.381145(29)	1518.4218(61)
$D_J^3 / \mathrm{kHz}$	0.168252(20)	0.1692	0.16462*	0.16462*
$D_{JK}^3  /  \mathrm{kHz}$	0.98347(48)	0.9915	0.94497(420)	0.94198(260)
$D_K^3 / \mathrm{kHz}$	0.31937*c,e		0.294*	0.294*
eQq <sub>3</sub> / MHz	-2146.49*b	-2146.49(11)		
		interactions		
$\sqrt{2}B_0\Omega\zeta_{36}^{(b)}$ / MHz	861.4*c	878.6*	903.7567(340)	1201.113(940)
$C_x^J/\mathrm{kHz}$			-0.79255(410)	-1.55868(720)
$C_x^K / \mathrm{kHz}$			-4.767(350)	-5.831(180)

<sup>\*</sup>Constrained values. aRef. <sup>29</sup>. bRef. 15.

°MP2 6-311G\*\*.

dRef. 14.

Ground state value.

fRef. <sup>17</sup>.

**Table 5.** Summary of errors in the global fit shown in Table 4.

Dataset	Description	No. of Transitions	Ave. Msmt Error	rms Fit Error
Ref. 18	IR data, $v_3$ fundamental	3053	$5.48 \times 10^{-4} \text{ cm}^{-1}$	$3.03 \times 10^{-4} \text{ cm}^{-1}$
Ref. 15	mm-wave, $J = 11-46$	441	259 kHz	273 kHz
Ref. 17	<i>l</i> -type doubling transitions	72	1.8 kHz	7.1 kHz
This work	J = 0-2	27	50 kHz	28 kHz

**Table 6.** Comparison of parameters derived from the fit (Table 4) with *ab initio* values obtained from the force field calculation

Parameters	This work	Ref. 15	Ref. 18, Calc. 2	Ref. 18, Calc. 3	MP2 6-311G**	CCSD 6-311G**	CCSD(T) 6-311G**
$D_J^0$ / kHz	0.16462*	0.16462(2)	0.16462*	0.16462*	0.1588	0.1580	0.1641
$D_{JK}^0 / \mathrm{kHz}$	0.9925*	0.9925(4)	0.9925*	0.9925*	0.8552	0.8611	0.8703
$D_K^0 / \mathrm{kHz}$	0.31937*		0.294*	0.294*	0.31937	0.3097	0.3100
$\alpha_6^{(A)}$ / MHz	-7.7166*	0*	0.42825*	-23.4747(24)	-7.7166	-7.864	
$\alpha_6^{(B)}$ / MHz	1.36254(21)	1.26	1.2048(1)	0.7251(31)	0.8424	0.8529	
$\zeta_{66}^{(a)}$	0.13765(9)	0.1367	0.1368*	0.1362*	0.1319	0.1319	0.1341
$\alpha_3^{(A)}$ / MHz	0.4254(3)	0*	0.4283(32)	0.4301(48)	0.4017	0.3747	
$\alpha_3^{(B)}$ / MHz	3.5822(3)	3.77	3.90153(3)	4.8609(61)	3.3487	3.2977	
$\zeta_{36}^{(b)}$	0.3996*	0.4076*	0.41928(2)	0.5570(4)	0.3996	0.3945	0.3963

<sup>\*</sup>Constrained value

### **Figures**

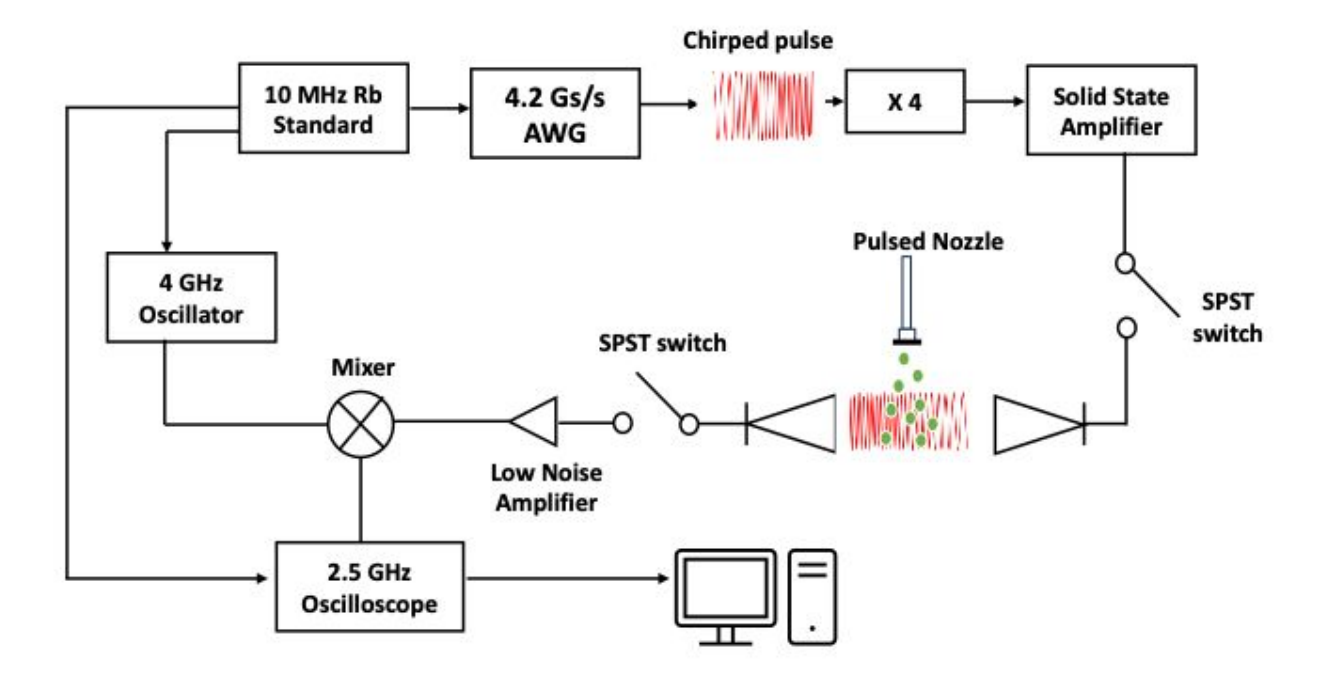
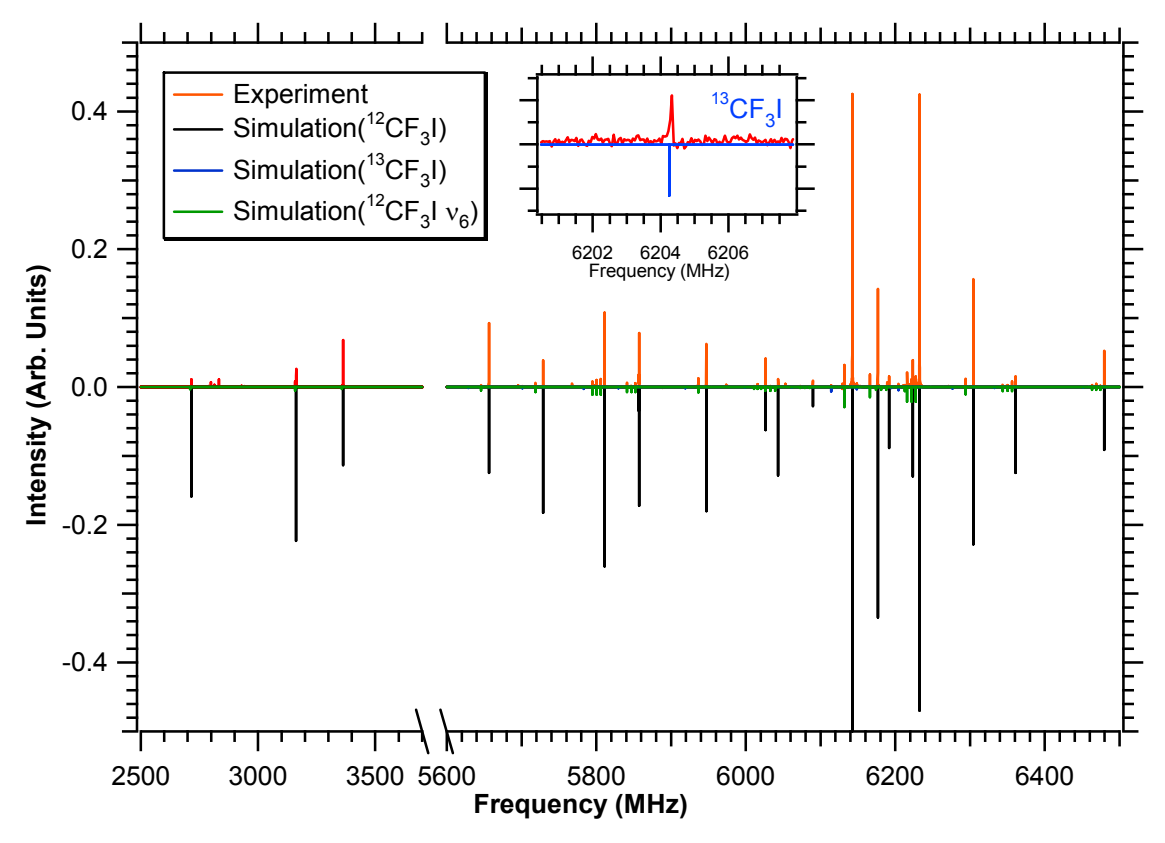
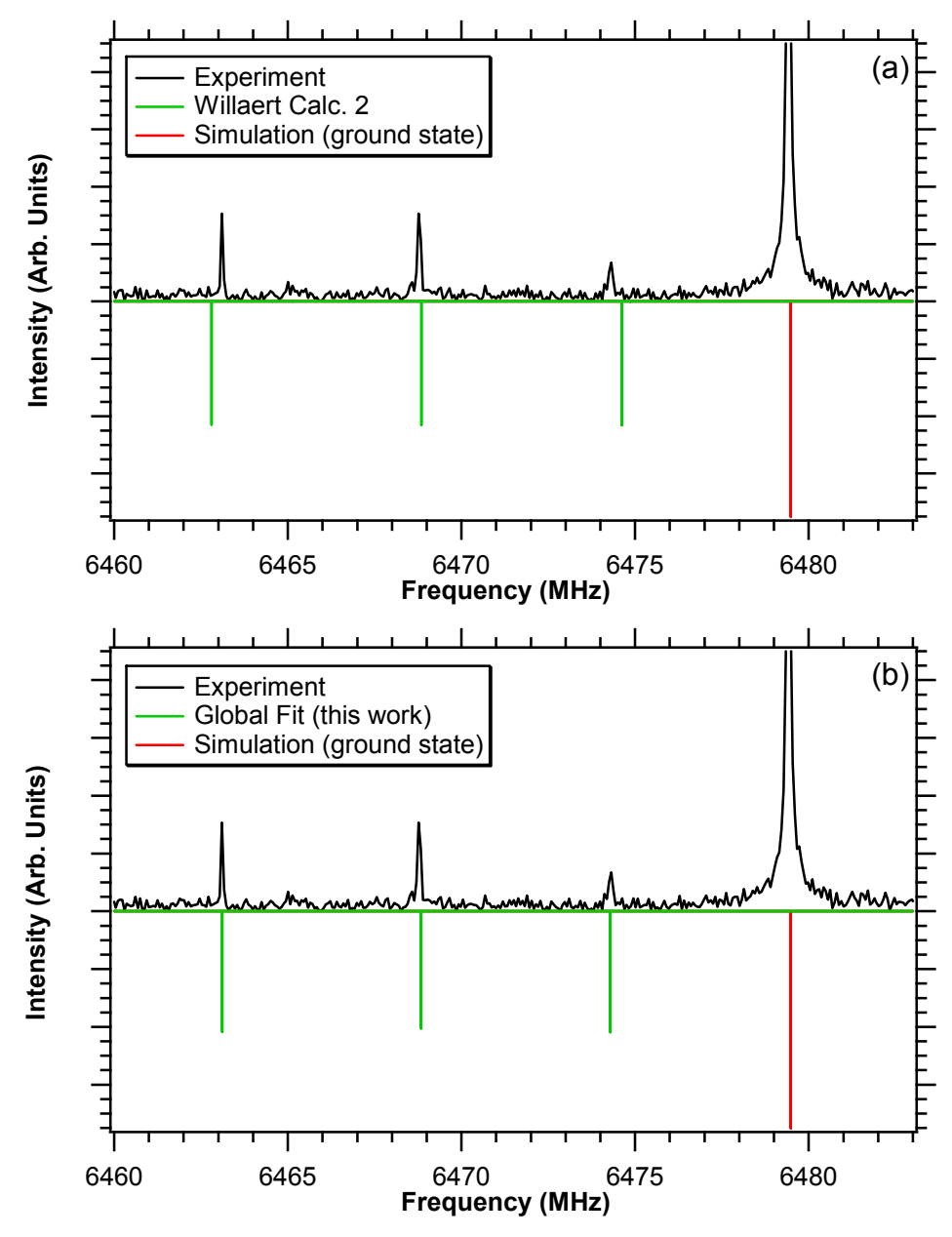


Figure 1. Schematic design of the 2-8 GHz CP-FTMW spectrometer



**Figure 2.** 2-8 GHz spectrum of CF<sub>3</sub>I. The spectrum contains lines in two different regions: J = 0 to 1 transitions lie in the 2500-3500 MHz range and J = 1 to 2 transitions lie in the 5600-6500 MHz range. The measured spectrum (red, upward directed peaks) is compared to simulated line frequencies and intensities (downward directed peaks, see legend). The inset shows the  $(J,K,F)=(2,1,4.5)\leftarrow(1,1,3.5)$  transition of the  $^{13}$ CF<sub>3</sub>I isotopologue, obtained in natural abundance.



**Figure 3.** The frequencies of the  $\nu_6$  vibrational satellites of the (J,K,F)=(2,1,0.5)  $\leftarrow$ (1,1,1.5) transition are compared to (a) simulated line positions calculated from the fit parameters reported in Calc. 2 of Willaert *et al.* <sup>18</sup> and (b) simulated line positions using the parameters reported in Table 4 of this work.

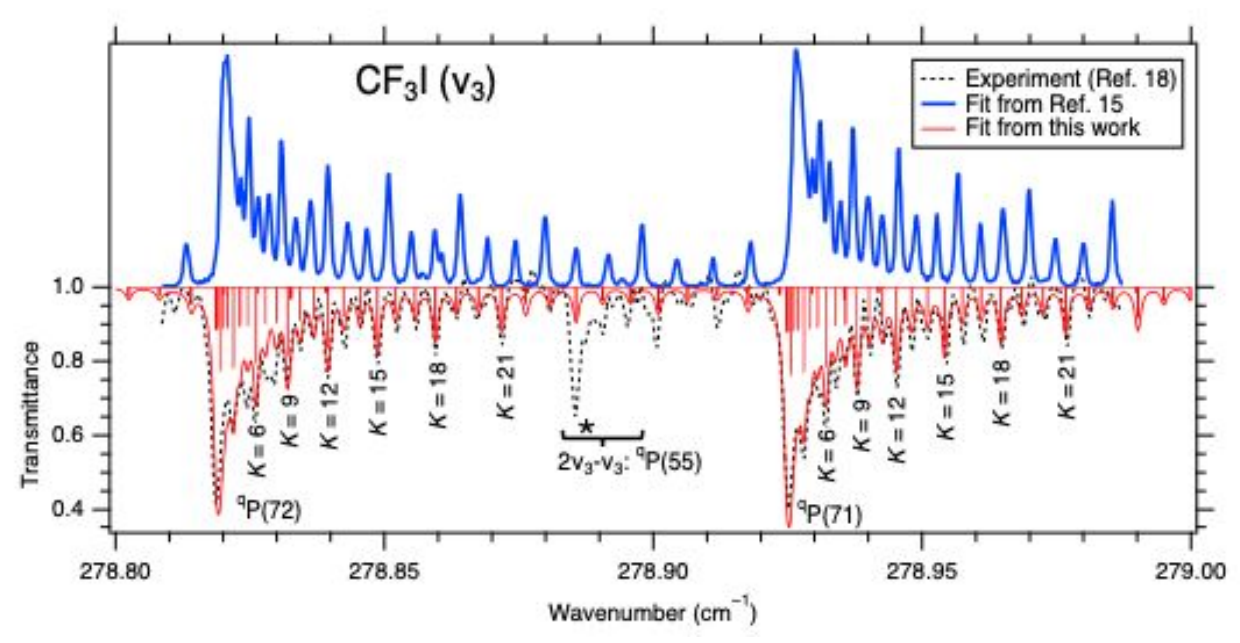


**Figure 4.** The recorded spectrum of the  ${}^qP(71)$  and  ${}^qP(72)$  branches of the  $\nu_3$  fundamental transition<sup>18</sup> (dotted line) is compared with the simulated spectra predicted by our fit (thin red line, downward directed peaks) and with the simulated spectrum predicted by the parameters of Walters and Whiffen<sup>15</sup> (thick blue line, upward directed peaks). The Walters and Whiffen prediction exhibits disagreement with the IR measurements at high J and high K because it is based on data that only extended to J = 41. Note that the feature at ~278.886 cm<sup>-1</sup> (marked with an asterisk) is due to the  $2\nu_3$ - $\nu_3$  hot band which is omitted from the fit model.

The data supporting this article have been included as part of the Supplementary Information.